Temperature coefficients of grain boundary resistance variations in a ZnO/p-Si heterojunction*

Liu Bingce(刘秉策), Liu Cihui(刘磁辉)†, Xu Jun(徐军), and Yi Bo(易波)

(Department of Physics, University of Science and Technology of China, Hefei 230026, China)

Abstract: Heteroepitaxial undoped ZnO films were grown on Si (100) substrates by radio-frequency reactive sputtering, and then some of the samples were annealed at N_2-800 ℃ (Sample 1, S1) and O_2-800 ℃ (Sample 2, S2) for 1 h, respectively. The electrical transport characteristics of a ZnO/p-Si heterojunction were investigated. We found two interesting phenomena. First, the temperature coefficients of grain boundary resistances of S1 were positive (positive temperature coefficients, PTC) while that of both the as-grown sample and S2 were negative (negative temperature coefficients, NTC). Second, the I–V properties of S2 were similar to those common p–n junctions while that of both the as-grown sample and S1 had double Schottky barrier behaviors, which were in contradiction with the ideal p–n heterojunction model. Combined with the deep level transient spectra results, this revealed that the concentrations of intrinsic defects in ZnO grains and the densities of interfacial states in ZnO/p-Si heterojunction varied with the different annealing ambiences, which caused the grain boundary barriers in ZnO/p-Si heterojunction to vary. This resulted in adjustment electrical properties of ZnO/p-Si heterojunction that may be suitable in various applications.

Key words: ZnO/p-Si heterojunction; grain boundary; temperature coefficients of grain boundary resistances; intrinsic defects

DOI: 10.1088/1674-4926/31/12/122001 **PACC:** 7155; 7340L; 7335

1. Introduction

Zinc oxide (ZnO) is wide band gap semiconductor ($\sim$ 3.37 eV at room temperature) with various applications, especially laser diodes (LDs) and light emitting devices (LEDs), and window material for display and solar cells[1]. However, ZnO is difficult to obtain as a high quality and reproducible p-type material, so practical device applications such as LDs and LEDs using ZnO are still experiencing inherent problems. In an alternative approach, various ZnO based heterojunction devices have been fabricated using different p-type substrates[2, 3].

The native ZnO is an insulator if it satisfies stoichiometry. However, the undoped ZnO shows typical n-type conductivity, which is attributed to structural defects. ZnO films depositing on a silicon substrate usually form a polycrystalline structure, so the grain boundary has a great influence on carrier transport[4]. The crystallization of ZnO films will be improved after annealing, but the dependence of electrical properties upon grain boundaries in ZnO/Si heterostructure annealing at various ambiences has not yet been well established. Any application of such a device therefore requires a thorough knowledge of the underlying phenomena.

In this study, we utilize current–voltage (I–V) and deep level transient spectroscopy (DLTS) measurements to investigate the variations of grain boundary annealing at the different ambiences and its influence on electrical properties of ZnO/p-Si heterojunction.

2. Experimental

2.1. Preparation of samples

ZnO films were deposited on some p-type Si (100) substrates by RF reactive sputtering. The p-Si substrates have a resistivity of 2–3 Ω·cm. At first, these substrates were carefully cleaned by CCl_4, toluol, acetone, ethanol, aqua fortis, hydrofluoric acid and deionized water in sequence. Then substrates were exposed to a dry N_2 flow. The target was a sintered oxide ceramic disk of ZnO (purity 99.99%). The target–substrate distance was 8 cm. Before deposition, the sputtering chamber was pumped down to 2×10^{-3} Pa. The working pressure was 2 Pa ($Ar : O_2 = 1 : 1$). An RF power of 6 W was applied to the ZnO target. No external bias voltage was applied to substrate. Then ZnO films were deposited on the Si substrates at 300 ℃ for 1 h. The thickness of the ZnO films was 200–300 nm. Lastly, some of the samples were annealed at N_2-800 ℃ and O_2-800 ℃ for 1 h, respectively.

2.2. Measurements

A DLTS signal is obtained from the NJ.M.DLTS deep level transient spectrometer in a temperature range of 77–350 K. A 0.01 Hz ultralow frequency sawtooth wave generator is used as the voltage source for I–V measurement. Indium is employed for the ohmic contacts. During electrical property measurement, the samples are kept in a dark chamber. More details about sample structure and electrical measurement apparatus can be founded in Ref. [5].

3. Results and discussion

As is well known, ZnO films depositing on silicon substrate usually form polycrystalline structures. When ZnO grains bond with the Si layer, the crystal boundary between them can be regarded as an intergranular boundary. So a large interfacial state existed at the ZnO/p-Si interface and ZnO grain boundaries due

* Project supported by the National Natural Science Foundation of China (Nos. 50472009, 10474091, 50532070).

† Corresponding author. Email: chliu@ustc.edu.cn

Received 6 June 2010, revised manuscript received 15 July 2010

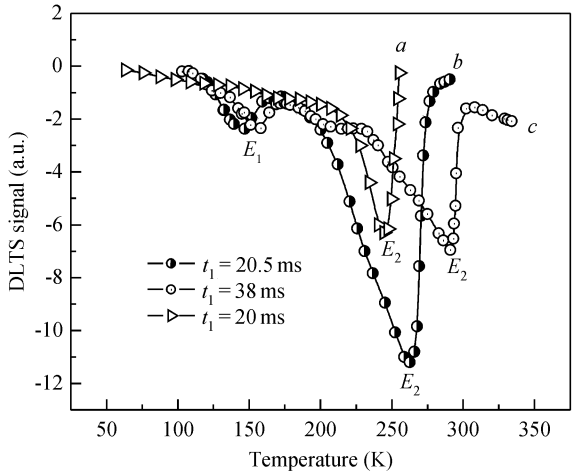

Fig. 1. DLTS spectra of annealed samples. (*a*) O_2-800 ℃ annealed, (*b*) unanneal and (*c*) N_2-800 ℃ annealed of samples.

to a large lattice mismatch. Also during sample preparation, the adsorption oxygen in the ZnO grain boundaries formed high densities of electron traps. They work together to give rise to the negative charge trapping at the grain boundaries. The negative charge must be compensated by a positive space charge double layer that extends into the interior bulk. Consequently, the Schottky barriers are formed. In polycrystalline ZnO films, the donor density near the surface is lower than that in the bulk, while near the ZnO/p-Si interface, the donor density is even lower. So the changes in depleted regions are mainly in ZnO grains adjacent to the grain boundaries, and the height of the barrier has a strong relationship with the concentration of deep level defects in the ZnO bulk. Here is Zn_i^{**}, is completed ionized zinc interstitials[6−8].

Figure 1 shows the DLTS spectrum of all samples measured at a certain rate windows. It is obvious that there are two deep level centers (E_1 and E_2) in the as-grown sample and S1. The trap centers at E_1 have almost disappeared in S2, but E_2 still exists.

Based on DLTS theory, the probability of electron emission e_n and the relative gap density N_t/N_B can be described as

$$e_n = \sigma_n V_{th} N_C \exp\left(-\frac{E_c - E_T}{kT_p}\right), \quad (1)$$

$$\frac{N_t}{N_B} = 2\frac{\Delta S_{max}}{\Delta C_{12}^*}\frac{\Delta V_r^*}{V_r}. \quad (2)$$

In Eq. (1), σ_n is the capture section of the deep level center, V_{th} is the average velocity of electron heat movement, N_c is the availability state density of the conducting band, $E_C - E_T$ is the distance between the electron trap energy and the conducting band, and T_p is the temperature of the corresponding electron trap energy level emission peak. In Eq. (2), ΔS_{max} is the DLTS spectrum peak value, ΔC_{12}^* is the DLTS signal calibration pulse which is the apparatus parameter, ΔV_r^* is the step pulse, V_r is the bias voltage, N_B is the concentration of substrate carries, and N_t is the concentration of electron trap centers.

Make an Arrhenius-plot of DLTS curves measured at different rate windows in Fig. 1 using Eq. (1). The location of the electron trap energy levels can be calculated from the curve slopes and the electron trap concentrations can be obtained from Eq. (2). The obtained DLTS results are listed in Table 1.

Table 1. DLTS properties of samples.

Sample	Energy level (eV)	N_t/N_B (%)
As-grown	$E_1 = E_C - 0.209$	2.76
	$E_2 = E_C - 0.718$	20.6
S1	$E_1 = E_C - 0.285$	0.75
	$E_2 = E_C - 0.793$	2.67
S2	$E_2 = E_C - 0.558$	0.83

It is clear that there are two deep level trap centers ($E_1 = E_C - 0.209$ eV and $E_2 = E_C - 0.718$ eV) in the as-grown sample. The first deep level, E_1 of 0.209 eV, has been reported many times and regarded as an electron trap energy level that related to Zn_i^{**}[8−11]. The second deep level, E_2 of 0.718 eV, has never been reported in other papers no matter whether ZnO films were deposited on sapphire or GaN substrates. We speculate that the origination of E_2 may be from the lattice mismatch between the Si substrate and ZnO film or the lattice damage caused by RF reactive sputtering. The details of this level need further research. The trap centered at E_1 almost vanishes after O_2-800 ℃ annealing but still exists after N_2-800 ℃ annealing.

Through the disordered layer at the grain boundary, there is a rapid grain boundary diffusion of oxygen as annealing at O_2 ambience. The rate of diffusion is enhanced by a high temperature. At the grain boundary, there is a reaction[11],

$$Zn_i^{**} + 2e' + \frac{1}{2}O_2(g) \Longleftrightarrow ZnO. \quad (3)$$

Thus a chemical potential gradient is established between the bulk and the grain surface, which provides the necessary driving force for the zinc interstitial diffusion. The net result is the creation of a thermodynamically stable ZnO lattice in the grain boundaries at the expense of reduction of $[Zn_i^{**}]$ ($[Zn_i^{**}]$ is the concentration of completed ionized zinc interstitials), which results in the improvement of the stoichiometric deviation of the ZnO grains. We believe this is the main reason that E_1 in S2 almost disappears after annealing at O_2-800 ℃[6].

As to the E_1 in S1, on the one hand the covered oxygen on the ZnO grain surface that formed during the sample preparation process began to desorption when annealed at N_2-800 ℃[10], these oxygen can diffuse into ZnO grains and recombine with Zn_i^{**}, which results in the reduction of $[Zn_i^{**}]$ in S1[11]. This is the reason that the relative gap densities of E_1 in S1 decrease a lot compared with that of the as-grown sample. On the other hand, as reported in Ref. [12], N_2 is an inert gas, a stable complex defect (Zn_i–N_O) is easily formed in ZnO grains, and the locations of the oxygen atom and the oxygen vacancy on the ZnO grain surface are easily replaced and occupied by a nitrogen atom, which results in the increment of $[V_o]$ in ZnO grain is confined ($[V_o]$ is the concentration of oxygen vacancy). This is favor to prevent the oxygen from diffusing into grains deeper, which means that the stoichiometric deviation of the ZnO grain cannot be much improved. This is the reason that $[Zn_i^{**}]$ of S1 is larger than that of S2, and the corresponding deep level center E_1 still exists after annealing at N_2-800 ℃. As to the location of E_1 in S1 moves deeper compared with that of the as-grown sample. We speculate that this is attributed to the regularization of the energy band caused by the variation

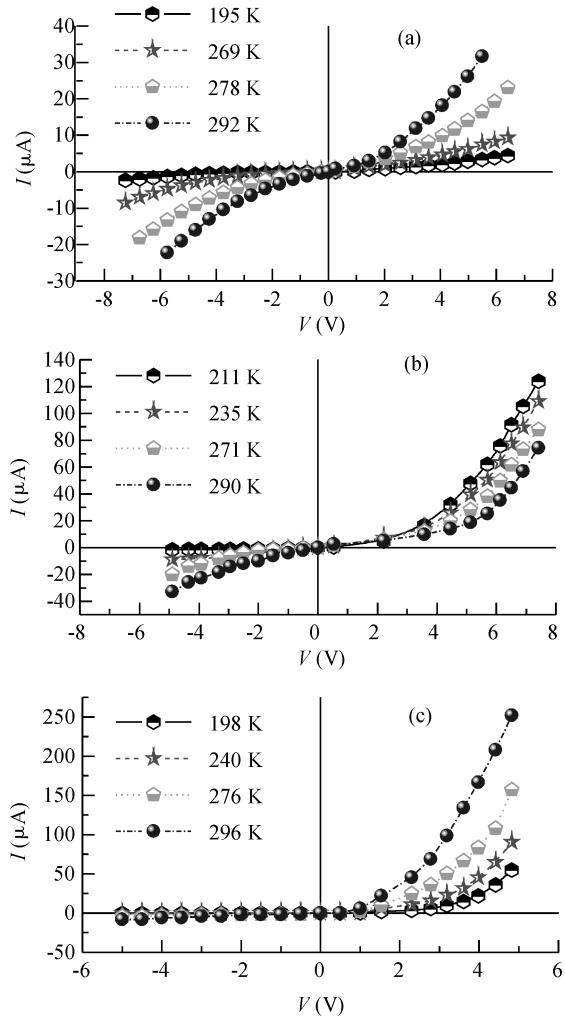

Fig. 2. I–V characteristics of all samples measured at various temperatures. (a) As-grown sample. (b) N_2-800 ℃ annealed. (c) O_2-800 ℃ annealed.

of $[Zn_i^{**}]$[12].

The I–V characteristics of all samples measured at various temperatures are shown in Fig. 2. Looking at Figs. 2(a) and 2(b), the I–V characteristics of both the as-grown samples and S1 exhibited a double-Schottky behavior with the measurement temperature rising. Considering the grain boundary effects in the ZnO/p-Si heterojunction, this is easily understood. As mentioned above, ZnO films depositing on silicon substrate usually form polycrystalline structures due to a large lattice mismatch, and a high density of interface states existed in the ZnO/p-Si heterojunction. In such a case, the p–n heterojunction can be regarded as p-type and n-type Schottky barrier in serials, thus I–V characteristics are dominated by the broad gap semiconductor (ZnO) side completely[13].

In the reverse transport process of the as-grown samples, the electrons in p region inject the interface region by tunneling and cross grain boundary barrier with thermo-emission. The tunneling probability increases with reverse voltages rising. The effective concentration of the carriers in the ZnO grains equals the product of the concentration of carriers that can inject into the interface region by tunneling, and the probability of those carriers that can cross grain boundary barrier by thermo-emission. This probability can be described by $P = \exp[-(e\varphi)/kT]$ using a Boltzmann distribution, where $e\varphi$ is the height of grain boundary barrier. Therefore, the temperature parameter decides the number of carriers that can cross the ZnO grain boundary directly. Investigate one of the I–V curves in Fig. 2(a), whose measured temperature is 195 K. In this situation, the probability of those carriers that can cross the grain boundary is small because the measurement temperature is low, which causes reverse currents to be near zero. This probability increases rapidly with the measurement temperature rising, which leads to reverse currents varied with various measured temperatures. So transport currents at reverse bias voltages increase dramatically with the measurement temperature rising, which results in current transports in the ZnO/p-Si heterojunction exhibiting a double-Schottky behavior. This is the same reason for the reverse I–V characteristics of S1.

Table 2. Variations of grain boundary resistances of all samples.

T (K)	$R_{\text{as-grown}}$ (kΩ)	T (K)	R_{s1} (kΩ)	T (K)	R_{s2} (kΩ)
195	960	211	29.4	198	30.4
269	588	235	32.2	240	20.9
278	206	271	37.3	276	15.9
292	110	290	40.7	299	11.2

The characteristic of I–V can be expressed as[13]

$$\begin{aligned} I &= SA^{**}T^2 \exp(-q\varphi_0/kT)\,[\exp((qV - IR_S)/nkT)] \\ &= I_0\,[\exp((qV - IR_S)/nkT)], \end{aligned} \tag{4}$$

$$I_0 = SA^{**}T^2 \exp(-q\varphi_0/kT), \tag{5}$$

where S, A^{**}, φ_0, n, R_S, T, k and I_0 are the heterojunction area, the Richardson's constant, the Schottky barrier height, the ideality factor, the series resistance, the Kelvin temperature, the Boltzmann constant and the saturated drain current, respectively. The R_S can be calculated by fitting I–V data in Fig. 2 using the first derivative of Eq. (4) for $q(V - IR_S) \geqslant 3nkT$[13]. The obtained results are listed in Table 2. Considering that ZnO films deposited on Si substrate form polycrystalline structures due to a large lattice mismatch, R_S is mainly attributed to grain boundary resistances[8].

It is obvious that the temperature coefficients of grain boundary resistances of S1 are positive while that of both the as-grown sample and S2 are negative, as shown in Table 2.

The variation in grain boundaries resistances of the as-grown samples can be easily clarified. During the fabrication process, there is a thin amorphous layer formed between the ZnO layer and the Si substrates due to lattice damage caused by RF reactive sputtering[14]. So there is a high density of interfacial states existing between the ZnO layer and the Si substrates.

A high density of interfacial states will cause the conduction band of ZnO to bend down largely and result in a large number of local recombination centers[15]. In the forward transport process of the as-grown samples, electrons are assumed to tunnel through a series of closely packed local recombination centers to reach the ZnO/p-Si interface from the conduction band of the ZnO, and then those electrons can jump into p region by thermo-emission directly[16].

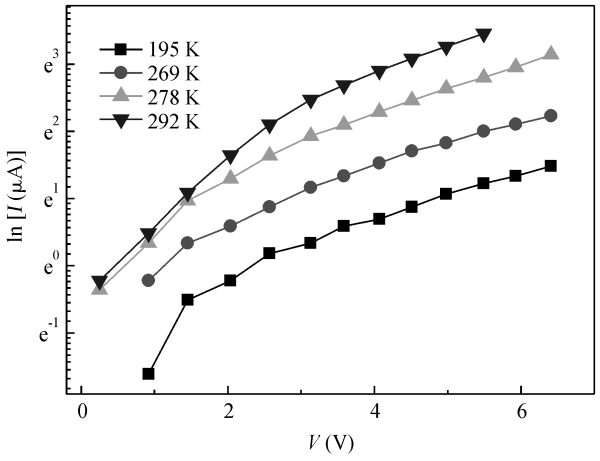

Fig. 3. Arrhenius-Plot of characteristics of as-grown sample.

The temperature-dependence of the forward I–V characteristics of the as-grown samples is shown in Fig. 3. It is obvious that the curves are almost parallel as voltages are above 2 V. This observation suggests that the forward electron transport is a tunneling mechanism via recombination centers[16]. So the number of electrons that can come into the p region is larger with the measurement temperature rising, which causes the forward current to become larger with the measurement temperature rising. This is the main reason that the NTC of the grain boundary resistances of as-grown samples appears.

Consider after N_2-800 ℃ annealing, the variation of grain boundary resistances of S1 can be explained easily.

The lattice damage caused by RF reactive sputtering and lattice mismatch between the ZnO layer and the Si substrates will be improved after N_2-800 ℃ annealing, but the stoichiometric deviation of the ZnO grain cannot be improved greatly, as mentioned above. So the influence of interfacial states between the ZnO layer and the Si substrates is impaired, while the ZnO grain boundaries still have large effects.

In this situation, as suggested by Heywang[17, 18], the PTC of resistances usually appears in polycrystalline metal oxide semiconductors, which have a high density of interfacial states between grains, and can be explained by the double Schottky barrier model. According to his explanation, in the grain bulk adjacent to grain boundaries, the negatively charged interfacial states are compensated by positively charged donor centers (here Zn_i^{**}) and a depletion space charge layer is formed. The presence of grain boundary acceptor states in this region results in the Fermi level lowering at the grain boundaries. To align the Fermi level across the interface, band bending occurs and a potential barrier between two grains is formed. The height of the potential barrier is strongly governed by the temperature and gives rise to the PTC resistance effect.

Using Heywang's model, the potential barrier φ_0 and barrier width d are

$$\varphi_0 = \frac{qN_S(T)}{[8\varepsilon_0\varepsilon n]}, \tag{6}$$

$$d = N_s/2n. \tag{7}$$

Here, $N_S(T)$ is the temperature-dependent density of the occupied acceptor states, n is the charge density in the grain, and ε is the relative dielectric constant in the depletion layers.

In view of the above, $N_S(T)$ decreased with the decrement of measurement temperature for the number of occupied acceptor states are less when the measurement temperature is low as some of the interfacial acceptor states are not activated[19]. So φ_0 and d reduce with the measurement temperature decreased, and the densities of current that flow through the grain boundaries are larger at the lower measurement temperature, which gives rise to PTC of the grain boundary resistances.

The NTC resistances of S2 are also easily explained. As mentioned above, the barrier height has a close relationship with $[Zn_i^{**}]$, as Zn_i^{**} is the ionized donor impurity in the depleted regions adjacent to the boundary. After O_2-800 ℃ annealing, the decrement of corresponding $[Zn_i^{**}]$ can be attributed to the interstitial zinc and oxygen recombination. In addition, oxygen diffuses into the interface of the ZnO/p-Si heterostructure as a high temperature annealing at O_2 ambience and then forms Si–O bonds there, which reduces the number of dangling bonds effectively that are caused by lattice mismatch[20]. So the height of the grain boundary barrier decreases as well as the densities of the interface states. The reasons mentioned above working together impair the influence of the grain boundaries and the interfacial states, which results in the double Schottky barrier behaviors disappearing. The transport mechanism of S2 can be described using a thermo-emission model. So the kinetic energy of the electrons increased with the measurement temperature rising, which results in the number of electrons that can cross over the barriers increasing, and the appearance of the NTC of the grain boundary resistance.

The reasons discussed above suggest that the variation of the grain boundary resistances is controlled by the densities of the interfacial states completely. After O_2-800 ℃ annealing, the microstructures of the ZnO/p-Si heterostructure are improved, and the influences of both the interfacial states and the grain boundaries are weakened.

4. Conclusion

The characterization of carrier transport in the ZnO/p-Si heterostructure and its temperature coefficients of resistance are investigated using I–V and DLTS measurements. The variations in temperature coefficients of the grain boundary resistances can be explained using the change of grain boundary behavior and the densities of the interfacial states. After O_2-800 ℃ annealing, the lattice mismatch and stoichiometric deviation of the ZnO grain are much improved, which results in the disappearance of the double-Schottky behavior and the appearance of the NTC resistances. This resulted in the adjustment of the electrical properties of the ZnO/p-Si heterostructures that may be suitable in various applications.

References

[1] Lee J Y, Jang B R, Lee J H, et al. Characterization of low mole fraction In-doped-ZnO/Si (111) heterostructure grown by pulsed laser deposition. Thin Solid Films, 2009, 517: 4086

[2] Qi H X, Li Q S, Wang C F, et al. Effects of oxygen pressure on n-ZnO/p-Si heterojunctions fabricated using pulsed laser deposition. Vacuum, 2007, 81: 943

[3] Chuang R W, Wu R X, Lai L W, et al. ZnO-on-GaN heterojunction light-emitting diode grown by vapor cooling condensation

technique. Appl Phys Lett, 2007, 91: 231113
[4] Fu Z X, Lin B X, Zu J. Photoluminescence and structure of the ZnO films deposited on Si substrates by metal-organic chemical vapor deposition. Thin Solid Films, 2002, 402 (1/2): 302
[5] Liu C H, Chen Y L, Lin B X, et al. Electrical properties of ZnO/Si heterostructure. Chin Phys Lett, 2001, 18(8): 1108
[6] Bernasconi J, Klein H P, Knecht B, et al. Investigation of various models for metal oxide varistors. J Electron Mater, 1976, 5(5): 473
[7] Mantas P Q, Baptista J L. The barrier height formation in ZnO varistors. Journal of the European Ceramic Society 1995, 15: 605
[8] Liu B C, Liu C H, Fu Z X, et al. Effects of grain boundary barrier in ZnO/Si heterostructure. Chin Phys Lett, 2009, 26(11): 117101
[9] Zhang S B, Wei S H, Zunger A. Intrinsic n-type versus p-type doping asymmetry and the defect physics of ZnO. Phys Rev B, 2001, 63: 075205
[10] Liu C H, Xu X Q, Zhong Z. Donor-acceptor luminescence in ZnO:LiCl/p-Si films. Chinese Journal of Semiconductors, 2007, 28(Suppl): 171 (in Chinese)
[11] Fan J, Freer R. Deep level transient spectroscopy of zinc oxide varistors doped with aluminum oxide and/or silver oxide. Journal of the American Ceramic Society, 1994, 77(10): 2663
[12] Look D C, Farlow G C, Reunchan P, et al. Evidence for native-defect donors in n-type ZnO. Phys Rev Lett, 2005, 95: 225502
[13] Sharma B L. Metal–semiconductor Schottky barrier junctions and their applications. New York, London: Plenum Press, 1984
[14] Lee H S, Lee J Y. Formation mechanism of preferential c-axis oriented ZnO films grown on p-Si substrates. J Mater Sci, 2004, 39: 3525
[15] Tuller H L. ZnO grain boundary: electrical activity and diffusion. J Electroceram, 1999, 4: S1, 33
[16] Bindal A, Wachnik R, Ma W. Observation of recombination center-assisted tunneling current in Al(Cu)-penetrated PtSi Schottky barrier diodes. J Appl Phys, 1990, 68: 6259
[17] Heywang W. Bariumtitanat als sperrschichthalbleiter. Solid-State Electron, 1961, 3: 51
[18] Ihrig H, Puschert W. A systemic experimental and theoretical investigation of the grain-boundary resistivities of n-doped $BaTiO_3$ ceramics. J Appl Phys, 1977, 48: 3081
[19] Sze S M. Physics of semiconductor devices. New York: Wiley, 1983
[20] Kang X H, He S H, Sang B S. Electrical properties and annealing effects of MZOS structure. Chinese Journal of Semiconductors, 1997, 18(12): 926 (in Chinese)